JOURNAL OF THEORETICAL
AND APPLIED MECHANICS
3, **40**, 2002

MODELING OF SMART COMPOSITE SHELL STRUCTURES

Ulrich Gabbert
Heinz Köppe
Falko Seeger
Harald Berger

Institute of Mechanics, University of Magdeburg, Germany
e-mail: ulrich.gabbert@mb.uni-magdeburg.de

Recently, thin piezoelectric foils or fibers with a thickness between 10 μm and 30 μm have been manufactured and used as sensor/actuator components of smart composite structures. The paper deals with the mathematical analysis and numerical simulation of such smart composite structures. A concept for laminated thin finite shell elements with active and passive layers considering three different approaches is introduced. In a test case the applicability of these different approaches is investigated and discussed. To verify the suitability of the algorithm for analyzing composite structures a practical example of a composite consisting of piezoelectric fibers embedded in a matrix material is considered. At first, the introduced composite shell elements are used, where the piezoelectric fibers are modeled as active layers in a smeared form. At second, a discrete concept is used, where the piezoelectric fibers are modeled as one-dimensional truss-like finite elements which are embedded into conventional finite elements by the penalty technique. These two approaches are discussed and compared.

Key words: smart shell composites, piezoelectric foils, piezoelectric fibers, finite element analysis

1. Introduction

Over the past few years the smart structures concept has been given increasing attention in many branches of engineering, and several novel engineering applications have been developed. Smart structures, or to be more precise structronic (structure + electronic) systems, are characterized by synergistic

integration of active materials into a passive structure connected by a control system to enable an automatic adaptation to changable environmental conditions. Piezoelectric materials (e.g. PZT, PVDF) are widely used as distributed sensors and actuators in smart structures, where especially hybrid composites – a combination of fiber-reinforced angle-ply and piezoelectric laminae – are very powerful smart material systems (Chee et al., 1998; Köppe et al., 1998, Gabbert and Weber, 1999; Sporn and Schoenecker, 1999). Such hybrid composites are characterized by a high structural conformity preventing major disturbances of the mechanical behavior as a result of the integration of actuator and sensor materials into the structure. In general the active material forms an integral part of a load bearing structure itself and does not cause significant changes in the passive behavior of the structure.

In vibration control of structures commercially available piezoelectric wafers (e.g. PI Ceramic, Germany; ACX, USA, etc.) are very common active materials. Such thin wafers are glued on the surface of the base structure or can be embedded in a composite during production.

It is very time-consuming and expensive to measure the macroscopic (homogenized) material data which are non-linear functions of the properties as well as the arrangement and the volume fraction of constituents in the composite. Alternatively, analytical methods (e.g. based on the Mori-Tanaka mean field approach) as well as numerical methods (e.g. based on the finite element analysis of a representative volume element) can be employed to calculate homogenized material tensors of a heterogeneous material system (Gabbert and Weber, 1999; Levin et al., 1999).

Powerful simulation tools are required for the analysis and the design process of complex engineering smart structures with integrated piezoelectric wafers and fibers as actuators/sensors. Here, the finite element method (FEM) provides an effective technique. Due to its wide-spread use it has become a theoretically and practically established method for a wide range of applications. It is also proved to be a suitable method for solving coupled piezoelectric field problems (Berger et al., 1999). Over the past years significant progress has been made in the development of finite elements for coupled electromechanical fields, but even today only special continuum finite elements are available in general purpose finite element codes, such as ABAQUS and ANSYS (Lin et al., 1994). Consequently, we developed a general purpose finite element simulation and design tool for piezoelectric controlled smart structures. The basis of this development was the standard software package COSAR (COSAR, 1992). The main new features are an extended library of multifield finite elements with coupled thermoelectromechanical degrees of freedom

(*dof*'s), a substructure technique which allows one to separate passive structures and structures with coupled electromechanical *dof*'s, numerical routines to solve static and dynamic problems, where also control algorithm and optimization tools for optimizing the actuator/sensor placement can be included (Berger et al., 1999; Görnandt and Gabbert, 2002; Gabbert and Weber, 2000). Controller design tools such as *Matlab/Simulink* can be applied via a standard data interface (Berger et al., 2001, Gabbert et al., 2001). New graphical features, e.g. description of material properties, application of electric loads, graphical representation of electric field values, etc., were added to provide a user-friendly simulation and design software.

In the following, a brief review of general theoretical fundamentals of our coupled electromechanical finite element analysis is given first. Then a concept for modeling thin piezoelectric composite structures is presented, where each active layer consisting of piezoelectric wafers or fiber bundle embedded in a matrix material is modeled as an anisotropic coupled electro-mechanical continuum and analyzed by a recently developed layered thin shell finite element. For comparison an alternative discrete concept is used, where the piezoelectric fibers are modeled as one-dimensional truss like finite elements which are embedded into 3D finite elements by a penalty technique.

2. General piezoelectric finite element formulation

The coupled electromechanical behavior of a polarizable (but not magnetizable) piezoelectric smart material can be modeled with sufficient accuracy by means of linearized constitutive equations. These linear equations can be derived from an energy expression (Tiersten, 1969) in a quadratic form of the primary field variables, i.e. mechanical strain $\boldsymbol{\varepsilon}$ and electric field $\boldsymbol{E}$, on the assumption that the temperature distribution $\overline{\theta}$ is *a priori* known or can be calculated independently of the electromechanical field. This results in the following constitutive equations

$$\begin{aligned} \boldsymbol{\sigma} &= \mathbf{C}\boldsymbol{\varepsilon} - \mathbf{e}\boldsymbol{E} - \boldsymbol{\zeta}\overline{\theta} \\ \boldsymbol{D} &= \mathbf{e}^{\top}\boldsymbol{\varepsilon} + \boldsymbol{\kappa}\boldsymbol{E} + \boldsymbol{\pi}\overline{\theta} \end{aligned} \tag{2.1}$$

In a compact form the equations (2.1) can be written as

$$\boldsymbol{\Psi} = \mathbf{J}\boldsymbol{\gamma} - \overline{\boldsymbol{\Theta}} \tag{2.2}$$

with

$$\boldsymbol{\Psi}^\top = [\boldsymbol{\sigma}^\top, \boldsymbol{D}^\top] \qquad \boldsymbol{\gamma}^\top = [\boldsymbol{\varepsilon}^\top, -\boldsymbol{E}^\top] \qquad \overline{\boldsymbol{\Theta}}^\top = [\boldsymbol{\zeta}^\top \overline{\theta}, -\boldsymbol{\pi}^\top \overline{\theta}]$$

and the stress vector $\boldsymbol{\sigma}^\top = [\sigma_{11}, \sigma_{22}, \sigma_{33}, \sigma_{12}, \sigma_{23}, \sigma_{31}]$, the strain vector $\boldsymbol{\varepsilon}^\top = [\varepsilon_{11}, \varepsilon_{22}, \varepsilon_{33}, 2\varepsilon_{12}, 2\varepsilon_{23}, 2\varepsilon_{31}]$, the electric field vector $\boldsymbol{E}^\top = [E_1, E_2, E_3]$, the $[9 \times 9]$ hypermatrix $\mathbf{J}$ containing the $[6 \times 6]$ elasticity matrix $\mathbf{C}$, the $[6 \times 3]$ piezoelectric matrix $\mathbf{e}$, and the $[3 \times 3]$ dielectric matrix $\boldsymbol{\kappa}$, the vector of thermal stress coefficients $\boldsymbol{\zeta}$, the temperature variation $\overline{\theta}$ of the body with respect to an initial temperature, the vector of electric displacements $\boldsymbol{D}^\top = [D_1, D_2, D_3]$, and the vector of pyroelectric coefficients $\boldsymbol{\pi}$. This general form is suitable to model any anisotropic behavior, e.g. smeared piezoelectric fiber layers or layers with interdigitated electrodes, etc.

The mechanical balance equations (Cauchy's equation of motion) $\sigma_{ij,j} + \overline{b}_i = \rho \ddot{u}_i$ and the electrical balance equation (4th Maxwell equation) $D_{i,i} = 0$ can also be written in a compact matrix form as

$$\mathbf{L}^\top \boldsymbol{\Psi} + \overline{\boldsymbol{b}} - \rho \ddot{\boldsymbol{q}} = \mathbf{0} \tag{2.3}$$

where $\boldsymbol{q}^\top = [\boldsymbol{u}^\top \phi]$ is the vector of generalized displacements including additionally the electric potential ϕ. Using the linear strain displacement relation $\varepsilon_{ij} = (u_{i,j} + u_{j,i})/2$, the relation between the electric field $\boldsymbol{E}$ and the electric potential $E_i = -\phi_{,i}$ which can be written in a matrix notation as $\boldsymbol{\gamma} = \mathbf{L}\boldsymbol{q}$, and the constitutive equation (2.2), the balance equation (2.3) can be rewritten as $\mathbf{L}^\top \mathbf{J} \mathbf{L} \boldsymbol{q} - \mathbf{L}^\top \overline{\boldsymbol{\Theta}} + \overline{\boldsymbol{b}} - \rho \ddot{\boldsymbol{q}} = \mathbf{0}$. The mechanical stress boundary conditions and the electric charge boundary conditions can be written as $\overline{\boldsymbol{\tau}} - \boldsymbol{\tau} = \mathbf{0}$ on O_τ, with $\overline{\boldsymbol{\tau}}^\top = [\overline{\boldsymbol{t}}^\top \overline{Q}]$, where $\overline{\boldsymbol{t}}$, $\overline{Q}$ are the traction vector and the surface charge, respectively. Additionally, the boundary conditions of the primary variables, i.e. prescribed displacements $\overline{u}_i$ and the electric potential $\overline{\phi}$, have to be fulfilled. The balance equations together with the boundary condition can be written in a weak form as

$$\delta\chi = \int_V \delta \boldsymbol{q}^\top (\mathbf{L}^\top \mathbf{J} \mathbf{L} \boldsymbol{q} - \mathbf{L}^\top \overline{\boldsymbol{\Theta}} + \overline{\boldsymbol{b}} - \rho \ddot{\boldsymbol{u}})\, dV + \int_{O_\tau} \delta \boldsymbol{q}^\top (\overline{\boldsymbol{\tau}} - \boldsymbol{\tau})\, dO = 0 \tag{2.4}$$

In a finite element discretization the interpolation functions $\mathbf{N}(\boldsymbol{x})$ are used to approximate the primary field variables $\boldsymbol{q}$ elementwise by the nodal degrees of freedom (*dof*s) $\boldsymbol{q}_e$. In a matrix form these approximations can be written as $\boldsymbol{q}(\boldsymbol{x}, t) = \mathbf{N}(\boldsymbol{x}) \boldsymbol{q}_e(t)$. Application of the matrix differential operator $\mathbf{L}$ on $\boldsymbol{q}$ results in $\mathbf{L}\boldsymbol{q} = \mathbf{L}\mathbf{N}\boldsymbol{q}_e = \mathbf{B}\boldsymbol{q}_e$. Introducing the shape functions into the weak formulation Eq. (2.4) of the coupled field problem and following the standard

procedure (partial integration, Gauss integral theorem) the semidiscrete form of the problem can be derived as

$$\mathbf{M}_e\ddot{\boldsymbol{q}}_e + \mathbf{R}_e\dot{\boldsymbol{q}}_e + \mathbf{K}_e\boldsymbol{q}_e = \boldsymbol{F}_e \tag{2.5}$$

with

$$\begin{aligned} \mathbf{M}_e &= \int_{V_e} \mathbf{N}^\top \rho \mathbf{N}\, dV \qquad & \mathbf{K}_e &= \int_{V_e} \mathbf{B}^\top \mathbf{J}\mathbf{B}\, dV \\ \boldsymbol{F}_e &= \int_{V_e} \mathbf{N}^\top \boldsymbol{b}\, dV + \int_{V_e} \mathbf{B}^\top \overline{\boldsymbol{\Theta}}\, dV + \int_{O_e} \mathbf{N}^\top \overline{\boldsymbol{\tau}}\, dO \end{aligned} \tag{2.6}$$

Additionally, a velocity proportional damping is taken into account in Eq. (2.5). The finite element library for piezoelectric controlled smart structures developed on the basis of the above given equations includes solid elements, plane elements, axisymmetric elements, rod elements as well as special multilayer composite shell elements (Berger et al., 1999; Gabbert et al., 1999, 2000b; Köppe et al., 1998). The shape functions of the finite elements can be linear or quadratic and the isoparametric element concept was used to approximate the element geometry. The solid element family consists of a basic brick-type element (hexahedron) and some special degenerated elements derived by collapsing nodes. The curved quadrilateral and triangular thick multilayered shell elements were developed on the basis of the discrete layer theory (Köppe et al., 1998). These elements are more efficient compared to the conventional isoparametric 3D hexahedron elements. The solution of the fully coupled thermo-electro-mechanical three-field problem is reported in Görnandt and Gabbert (2002). Recently, we extended the finite element library by quadrilateral and triangular curved thin shell elements based on the classical Kirchhoff-Love hypothesis (see Section 3).

3. Piezoelectric composite shell structure concepts

3.1. Element formulation

The most effective technique to analyze thin-walled structures is the application of finite shell elements developed on the basis of the classical *Kirchhoff-Love* hypothesis. Among the huge amount of different types of thin shell elements in our FEM software COSAR the *SemiLoof* element family, originally

proposed by Irons (Irons, 1976) is preferred to solve complex engineering problems. This preference results from a long time of practical experiences in several fields of application, where the elements have shown good overall accuracy and robustness in comparison with other elements. Consequently, we selected the *SemiLoof* element for extension to a smart shell element. The element contains the displacements u, v, and w at all 8 nodes, and additionally, at the two *Gauss* integration points of the four edges rotations in tangential direction are introduced which are allocated to the mid-side nodes (i.e. a mid-side node has the *dof*'s u, v, w, ϑ_1 and ϑ_2). Two families of shape functions are defined for the finite element formulation. *Lagrangian* polynomials are used for the displacements and *Legendre* polynomials for the rotations. Due to the definition of the rotations and displacements the element includes 32 *dof*'s. The classical laminate theory is applied to simulate thin composite structures. Consequently, the stresses vary linearly over the thickness direction. To include the electromechanical coupling into this element we have developed three different approximations which result in the following element types:

Element $S1$**:** The electric influence is taken into account in terms of distributed forces and moments only.

Element $S2$**:** The difference of the electric potential of each active layer is taken into account as additional element *dof*'s (poling in normal direction).

Element $S3$**:** Each element node has as many additional electric *dof*'s as there are active layers in the composite (in-plane electric poling).

The test results demonstrate that in thin shell structures these elements provide sufficient accuracy in the analysis of the global structural behavior of smart piezoelectric composites at a drastically reduced total number of *dof*'s compared with a 3D analysis (see Seeger et al., 2001).

Element $S1$

In the first step the forces and moments on the edges of each active element are introduced to simulate the influence of the electric field at the structure. These equivalent forces and moments are calculated in such a way that they result in the same strain field as caused by the electric field. Only the electric field normal to the shell mid-surface is regarded because thin actuators with electrodes applied at the top and the bottom surface of an active layer are

considered here. Additionally, the electric field E_3 in the thickness direction z is assumed to be constant over the thickness h_i of the active layer i

$$E_{3i} = \frac{1}{h_i} \Delta\phi_i \tag{3.1}$$

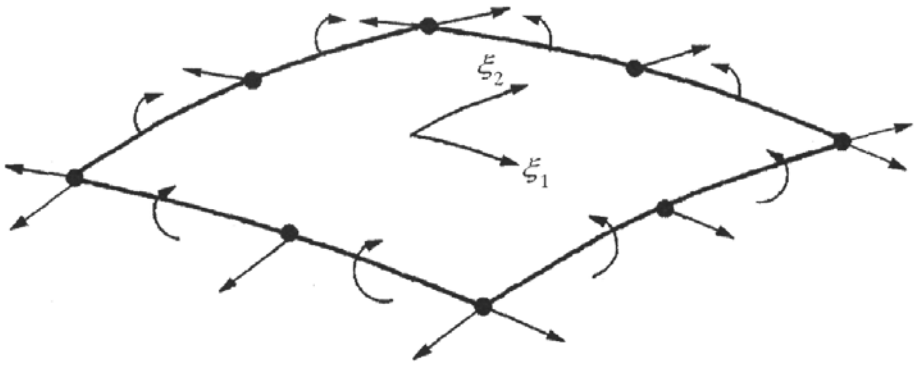

Fig. 1. Electric forces and moments of smart *SemiLoof* element $S1$

The integration of the element stresses over the thickness direction results in forces and moments which are oriented in the normal and tangential direction to the element edges, respectively. These forces and moments can be split into an electric and a mechanical part. Due to the above given assumption the electric part of the active layer results in membrane forces f_i only (see Figure 1). The reduction of these forces to the mid-plane of the shell results in additional moments. The electric membrane forces and the electric moments acting on the mid-plane of the element can be calculated as

$$\begin{aligned} \boldsymbol{f}_i &= -\int_z \mathbf{e}^\top \boldsymbol{E}_i \, dz = -\begin{bmatrix} e_{31} \\ e_{32} \\ 0 \end{bmatrix} \Delta\phi_i \\ \boldsymbol{m}_i &= \boldsymbol{f}_i z_i = -\begin{bmatrix} e_{31} \\ e_{32} \\ 0 \end{bmatrix} z_i \Delta\phi_i \end{aligned} \tag{3.2}$$

where z_i is the distance of the ith active layer $(i = 1, ..., n)$ from the mid-plane of the shell element. In this formulation no electromechanical interaction is included. The electric influence is only taken into account on the right hand side of equation of motion Eq. (2.5). The element stiffness matrix $\mathbf{K}_e$ of Eq. (2.6) consists of the original *SemiLoof* stiffness matrix only.

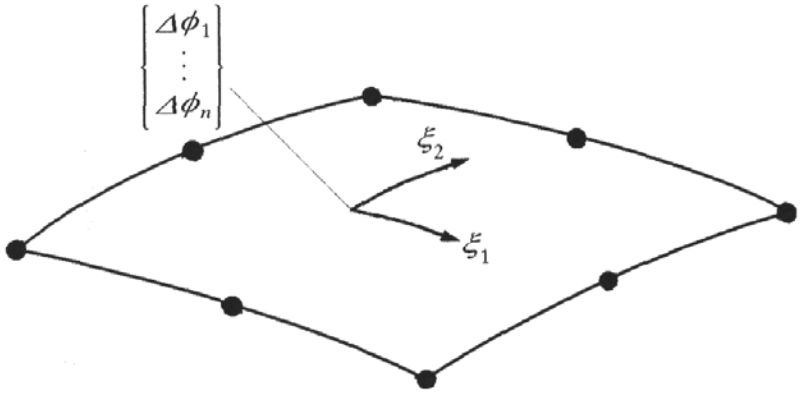

Fig. 2. Smart *SemiLoof* element $S2$

Element $S2$

In this extension of the *SemiLoof* element the electromechanical coupling is taken into account. In comparison to element $S1$, this results in an extension of the element stiffness matrix $\mathbf{K}_e$ as given in Eq. (2.6). The electric field is assumed to be the same as in element $S1$ which results in Eq. (3.1). Again, a complete metalized and electrodized surface of each active PZT element layer is assumed. The electric field is represented by the difference of the electric potential $\Delta\phi$ between the bottom and the top of the active layer, which is assumed to be constant over the whole active element layer, and consequently, no shape functions are required to approximate the electric field in the finite element. The element is enhanced by additional *dof*'s – electric potential differences $\Delta\phi_i$ – per each active layer i. These additional *dof*'s can be added to the midpoint of the element as given in Figure 2. The stiffness matrix of the extended *SemiLoof* element consists of the original pure mechanical stiffness matrix $\mathbf{K}_e^{(mm)}$ of the *SemiLoof* element, the new pure electric stiffness matrix $\mathbf{K}_e^{(ee)}$ and the coupling matrix $\mathbf{K}_e^{(me)}$ which can be derived on the basis of the classical *Lagrangian* finite element formulation as

$$\begin{bmatrix} \mathbf{K}_e^{(mm)} & \mathbf{K}_e^{(me)} \\ \mathbf{K}_e^{(me)\top} & \mathbf{K}_e^{(ee)} \end{bmatrix} \begin{Bmatrix} \boldsymbol{u}_e \\ \Delta\boldsymbol{\varphi}_e \end{Bmatrix} = \begin{Bmatrix} \boldsymbol{f}_e^{(m)} \\ \boldsymbol{f}_e^{(e)} \end{Bmatrix} \tag{3.3}$$

with

$$\mathbf{K}_e^{(mm)} = \int_{A_e} \mathbf{B}^{(m)\top} \mathbf{C} \mathbf{B}^{(m)}\, dA \qquad \mathbf{K}_e^{(me)} = \int_{A_e} \mathbf{B}^{(m)\top} \mathbf{e} \mathbf{B}^{(e)}\, dA$$
$$\mathbf{K}_e^{(ee)} = \int_{A_e} \mathbf{B}^{(e)\top} \boldsymbol{\kappa} \mathbf{B}^{(e)}\, dA \tag{3.4}$$

In Eq. (3.3) $\Delta\boldsymbol{\varphi}_e$ contains the voltage differences of each active element layer. Consequently, the quadrilateral *SemiLoof* element consists of $(32 + n)$ *dof*'s finally, where n is the number of active layers. It should be mentioned here, that also an improved version of this element type has been developed, implemented and tested, where we assumed a linear electric field distribution (rather than a constant one) via the thickness direction of the active layer (quadratic potential). But it could be shown that in thin shell applications the assumption of a constant electric field results in sufficiently accurate results (see Seeger et al., 2001). Consequently, this element is prefered due to the lower computational cost.

Element $S3$

Another way to couple the electric and the mechanical fields of the *SemiLoof* element is to neglect the field normal to the shell-midsurface and to simulate the field in the plane of the active layer only. In this case at each element node one electric *dof* per active layer has to be added. These additional eight *dof*'s per each active layer are used to approximate the distribution of the electric field in the ith layer by quadratic shape functions N_L

$$\Phi_i(\xi_1, \xi_2) = \sum_{L=1}^{8} N_L(\xi_1, \xi_2)\phi_{iL} \tag{3.5}$$

With these shape functions the electric part $\mathbf{B}^{(e)}$ of the matrix $\mathbf{B}$, which contains the derivatives of the shape functions with respect to the in-plane local co-ordinate system (x_1, x_2), can be calculated. The stiffness matrix is then calculated as given in Eqs. (3.3) and (3.4). This element has $(32 + 8n)$ *dof*'s in total, if n is the number of active layers (Figure 3). Element $S3$ was especially developed to analyze smart structures with interdigitated electrodes.

3.2. Comparison of elements

Three different types of active *SemiLoof* shell elements were presented in Section 3.1. These elements are based on the same basic shell element for the approximation of the mechanical field. But there are some differences regarding the approximation of the electric field. Comparing two elements $S1$ and $S2$, no differences can be observed if the actuator layer is driven by a given electric voltage. Element $S1$ can not be used to calculate the sensor voltage, because there is no direct coupling between the mechanical and the electric field. Of course, it is possible to calculate an electric potential caused

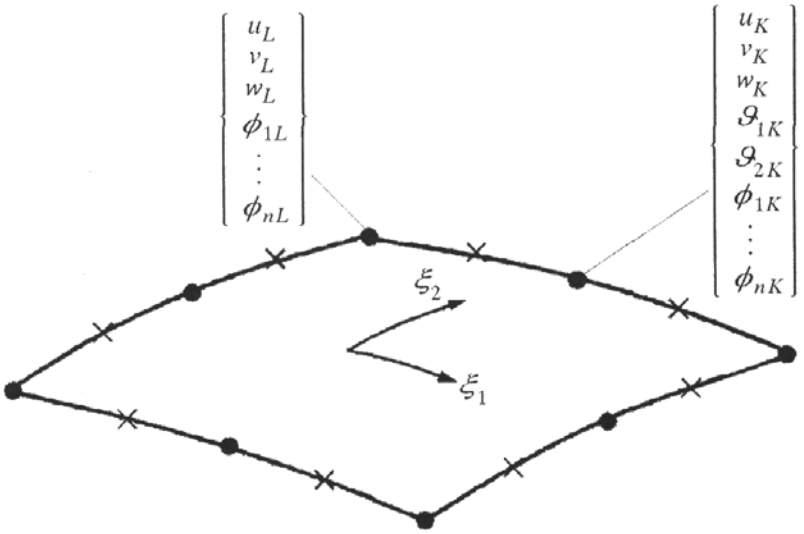

Fig. 3. Nodal degrees of freedom (*dof*'s) of smart *SemiLoof* element $S3$

by a given deformation, but without taking into account the coupling of the strain field and the electric field the calculated potential is higher than the real value calculated correctly by element $S2$. Element $S3$ was developed for applications, where the electric field is oriented parallel to the mid-plane of the shell. Such behavior is typical in active layers with interdigitated electrodes. It is possible to use elements $S1$ and $S2$ to simulate those structures too, but only to study global effects. Element $S3$ allows one to handle interdigitated electrodes directly and to study local effects. But here the main problem of the analysis is the unknown direction of the polarisation vector which can differ at each point of the structure. Of course, in principle, the polarisation vectors can be calculated by applying nonlinear models including the domain switching and domain wall changes under a high electric and mechanical field (Kamlah and Tsamakis, 1999). For the purpose of an approximate determination of the final poling direction a very simple approach is used here. At first, the electric potential alone is calculated in an isotropic dielectric medium. We assume that in an ideal case the vector of the poling direction at each point (we have used the integration points of the finite elements) corresponds with the direction of the gradient of the electric potential field. Finally, the material properties known for a given poling direction are transformed to the calculated new poling direction at each integration point. These data are then used in the calculation of the coupled electromechanical field.

In the following a simple test structure – a clamped plate (Figure 4) with a pair of bounded active layers (Gabbert et al., 1999, 2000b; Köppe et al., 1999) – is used to compare the new active thin shell elements with solid elements.

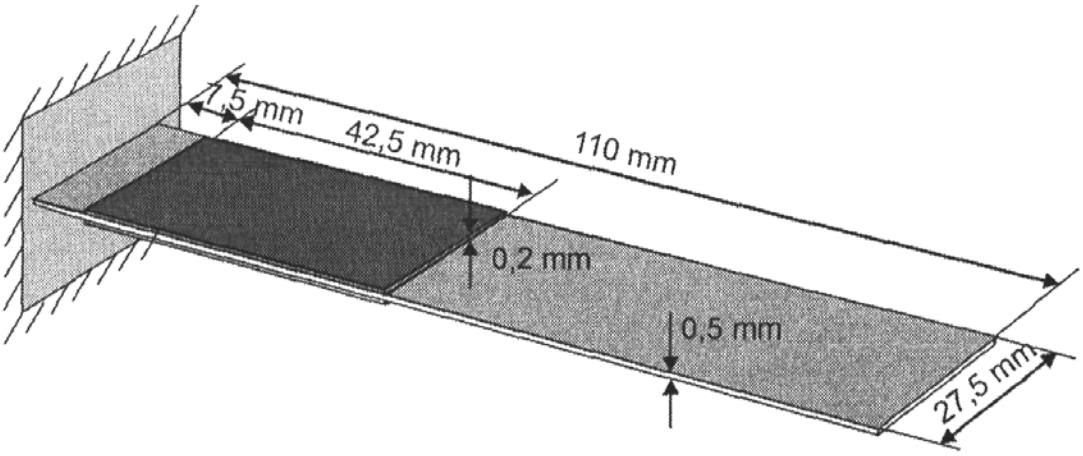

Fig. 4. Plate with applied actuators

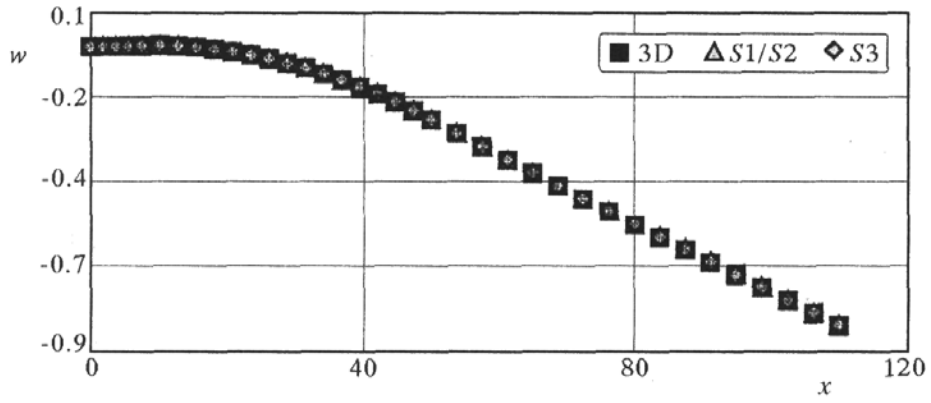

Fig. 5. Comparison of the shell and solid

The bending deformation results from contraction and elongation of the piezoelectric actuators glued at the upper and lower side of the plate. Figure 5 shows the deflection calculated with different element types. Table 1 shows the differences in the deflection of the tip of the plate. In the second investigation the thickness of the plate was varied. The results are shown in Fig. 6 and Fig. 7. These different approaches show very small variations in the results only. But, of course, the shell type solutions were calculated with a considerable lower amount of costs, because the preparation of the input data is much simpler and the computer time to calculate the solution is much less than in the 3D case due to a lower number of *dof*'s. This is mainly important in dynamic applications, where a time integration schema, such as the Newmark method, is used (see Seeger et al., 2001) to simulate the behavior of a smart structure in the time domain.

Table 1. Tip deflection of the plate

Element type	3D	$S1$	$S2$	$S3$
$u_3(x = 110\,\text{mm})$	$-0.8262\,\text{mm}$	$-0.8371\,\text{mm}$	$-0.8371\,\text{mm}$	$-0.8375\,\text{mm}$

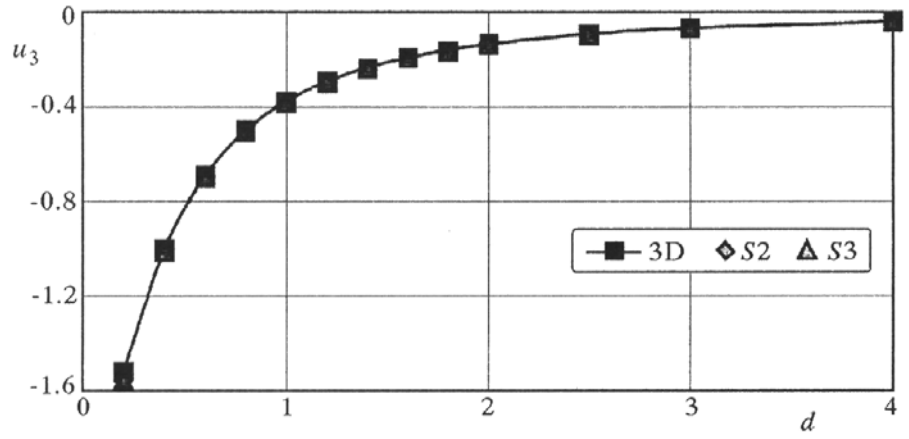

Fig. 6. Displacement at $x = 110\,\text{mm}$ as function of the plate thickness

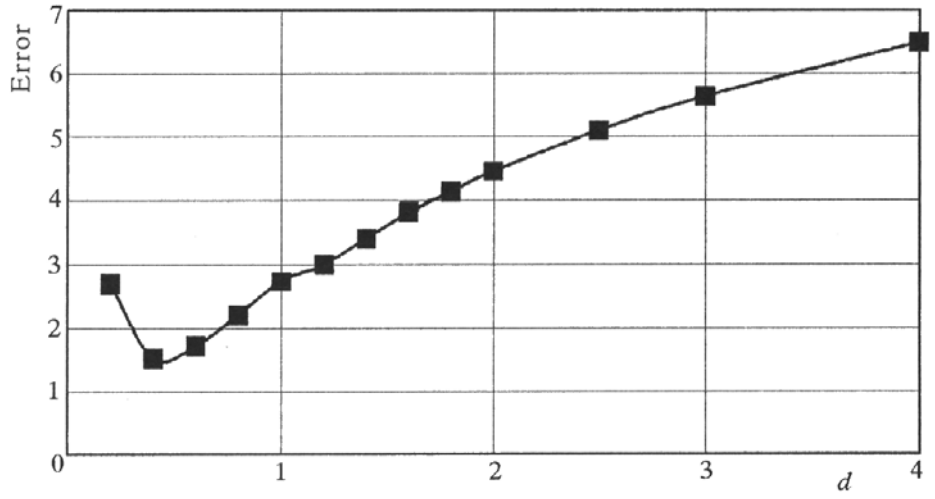

Fig. 7. Error between solid elements and element $S2$ as function of the plate thickness in %

4. Example of using composite shell elements for piezoelectric fiber structures

The discrete concept is useful for the simulation of problems with a low fiber volume fraction (*fvf*) and for an investigation of local structural effects (e.g. fracture, damage, delamination, etc.). In the following, 3D models are used to study piezoelectric fiber composites. We consider a structure containing a series of one-dimensional piezoelectric fibers embedded in the surrounding matrix material. As the passive matrix material preferably an epoxy resin is used which is assumed to be isotropic. The fibers may lie parallel to each other. By varying the distance between the single fibers different *fvf*'s can be achieved. In this way it is possible to adjust a special *fvf*, i.e. the volume percentage of the fibers related to the volume of the whole fiber/matrix compound structure. In our example we have chosen a relatively small *fvf* of about 6%. In this case the fibers are arranged in one layer and the main parameters of the cross-sectional area perpendicular to the fiber axis are: fiber diameter: 0.03 mm; distance between the single fibers: 0.0676 mm; thickness of the matrix material layer: 0.35 mm. At this point it is necessary to come to a further important constituent as a part of the above described compound structure – the so called interdigitated electrode. That means that we have to consider electrodes which consist of thin metal wires arranged in a comb-like shape (see Fig. 8). The adjacent wires have a distance of about 1 mm. Now we can imagine the whole compound structure in such a way that the fibers are aligned in the x_3 direction, whereas the thickness of the structure stretches in the x_2 direction. This is shown in a simplified manner in Figure 8.

In the numerical simulation we have compared the solutions between two discrete finite element models and one smeared concept with shell elements based on the models presented in Section 3. Both discrete element models are different by their various element approaches (linear and quadratic shape functions). The linear model consists of hexahedron elements with eight nodes and piezoelectric truss elements with two nodes whereas the quadratic model consists of hexahedron elements with twenty nodes and truss elements with three nodes. The passive hexahedron element has three *dof*'s per node (u_1, u_2, u_3) and the active truss element has four *dof*'s per node (u_1, u_2, u_3, ϕ). The fiber or truss elements were integrated into the matrix structure by assigning the edge nodes of the volume elements to the nodes of the truss elements by a penalty method. Furthermore, the electrodes were contacted to voltages of 100 V and 0 V, respectively. Displacement boundary conditions were introduced in the x_1x_2 plane. Figure 9 shows a characteristic section between two adjacent

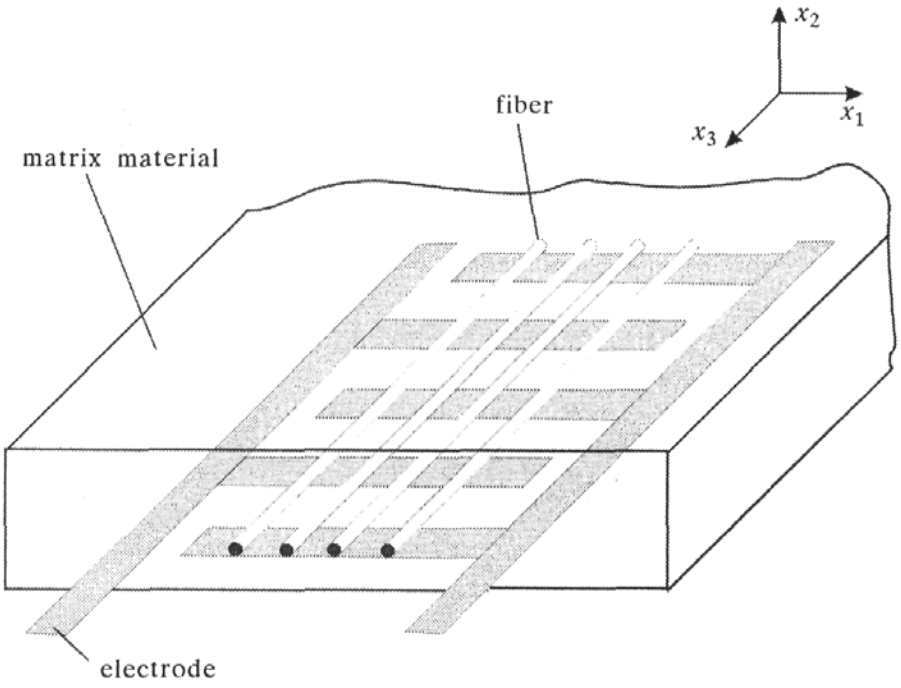

Fig. 8. Fiber/matrix composite with an array of interdigitated electrodes

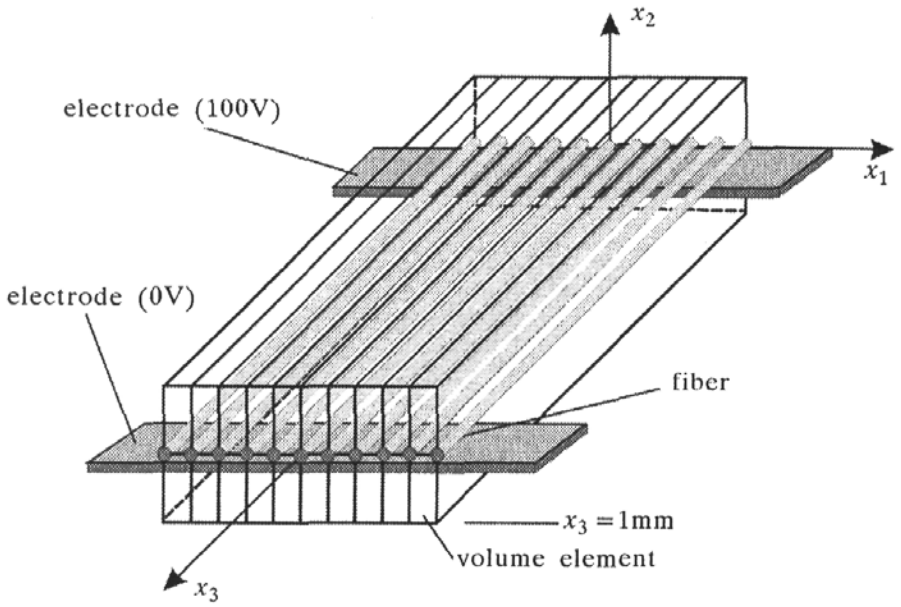

Fig. 9. Mechanical model of the fiber/matrix compound structure

electrodes of the finite element model. Over the thickness of the structure two rows of volume elements were arranged, each of them having half the thickness of the structure. The structure was divided into 240 hexahedron elements for the matrix material and 132 truss elements for the piezoelectric fibers. The resulting mesh is presented in Figure 10. To compare the results of the discrete method with the smeared concept the mesh with shell elements of type $S3$ (see Section 3.1) was prepared (see Figure 11).

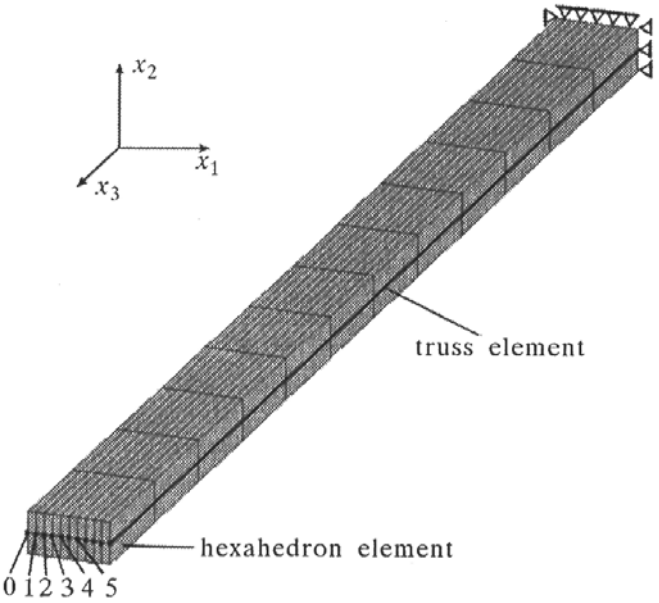

Fig. 10. Finite element mesh for the discrete model

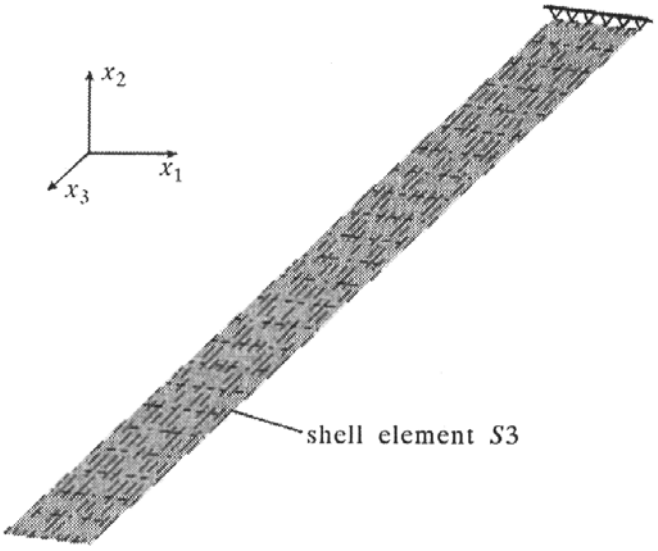

Fig. 11. Finite element mesh for the smeared model

Table 2 represents the displacements u_3 of the fiber ends. It can be seen that the displacement u_3 which describes the total length change of the fiber is almost constant over the whole range of the fibers regarded.

Table 2. Displacements of the fiber end points at $x_3 = 12\,\text{mm}$

Fiber No. i		0	1	2	3	4	5
Position x_1 [mm]		−0.3380	−0.2704	−0.2028	−0.1352	−0.0676	0
$u_3 \cdot 10^3$ mm	Linear model	0.1484	0.1479	0.1477	0.1476	0.1475	0.1475
	Quadratic model	0.1496	0.1485	0.1482	0.1481	0.1480	0.1480
	Smeared model	0.1381	0.1381	0.1381	0.1381	0.1381	0.1381

5. Conclusion

Recently, thin piezoelectric fibers with diameters between 10 μm and 30 μm have been manufactured and used as sensor/actuator components of smart composite structures. In the paper different approaches to simulate the active behavior of smart structures controlled by such active fibers are presented and compared. The basis of this investigation is the finite element simulation and design tool COSAR which has been extended to coupled electromechanical problems. A theoretical foundation of this extension is presented briefly. The main focus of the paper is on the modeling of piezoelectric fibers as a part of an active composite. At first a smeared concept is proposed, where each active layer consisting of piezoelectric fibers embedded in a matrix material is modeled as an anisotropic coupled electro-mechanical continuum and analyzed by special finite shell elements which have been developed recently on the basis of the classical *SemiLoof* element. Three different extensions of this shell element are presented and compared. Test examples demonstrate that thin composites controlled by voltage induced piezoelectric actuators can be modeled with sufficient accuracy by equivalent forces and moments. In sensor applications a direct electromechanical coupling is needed, where one additional electric *dof* per active element layer is sufficient. The homogenized material data which are required to model active layers in a composite have to be determined by measurements. The high effort of such measurements can be drastically reduced if additionally analytical and numerical methods are used, e.g. based on the mean field approach. Wafers with inerterdigitated electrodes can also be simulated with shell elements, where an additional electric *dof* per active layer is required at each element node. Thus, any in-plane distribution of the electric

field can be taken into consideration, where especially variable poling directions can be taken into account as well. Secondly, a discrete concept is used, where the piezoelectric fibers are modeled as one-dimensional truss like finite elements which are embedded into conventional finite elements by a penalty technique. Therefore, it is also very simple to vary the fiber volume fraction. It is shown that even in the case of small fiber volume fractions the accuracy of the smeared concept based on the shell theory results in a sufficient accuracy in comparison with a more expensive 3D analysis, where each fiber is taken into account by single truss elements. This approach is more interesting in the modeling of local effects such as fiber cracking or delamination.

Acknowledgement

This work is a part of the *Leitprojekt Adaptronik*, supported by the German Ministry for Science and Technology (BMBF), and the *Innovationskolleg* ADAMES, supported by the German Research Society (DFG). These supports are gratefully acknowledged.

References

1. BERGER H., GABBERT U., KÖPPE H., SEEGER F., 1999, Finite element analysis and design of piezoelectric controlled smart structures, *J. of Theoretical and Applied Mechanics*, 3, **38**, 475-498

2. BERGER H., KÖPPE H., GABBERT U., SEEGER F., 2001, On finite element analysis of piezoelectric controlled smart structures, in Gabbert U., Tzou H.-S. (Eds.): *Smart Structures and Structronic Systems*, Kluwer Academic Publisher, 189-196

3. CHEE C.Y., TONG L., STEVEN G.P., 1998, A review on the modelling of piezoelectric sensors and actuators incorporated in intelligent structures, *J. of Intelligent Material Systems and Structures*, **9**, 3-19

4. COSAR – General Purpose Finite Element Package: Manual, (1992), FEMCOS mbH Magdeburg (see also: http://www.femcos.de)

5. GABBERT U., BERGER H., KÖPPE H., CAO X., 2000a, On modeling and analysis of piezoelectric smart structures by the finite element method, *J. of Applied Mechanics and Engineering*, **5**, 1, 127-142

6. GABBERT U., GÖRNANDT A., KÖPPE H., SEEGER F., 1999, Benchmark problems for the analysis of piezoelectric controlled smart structures, *ASME 1999, Design Engineering Technical Conferences DETC'99*, Las Vegas, Nevada, September 12-16, 1999, paper: *DETC99/VIB-8391* (on CD-ROM)

7. GABBERT U., KÖPPE H., SEEGER F., 2001, Overall design of actively controlled smart structures by the finite element method, in Rao V.S. (Edit.): *Modeling, Signal Processing, and Control in Smart Structures, SPIE Proceedings Series*, vol. 4326, 113-122

8. GABBERT U., KREHER W., KÖPPE H., 2000b, Mathematical modeling and numerical simulation of smart structures controlled by piezoelectric wafers and Fibers, *Proceedings of the EUROMAT'99 Conference*, 27-30 September 1999, Munich, Wiley-VCH, **13**, 525-530

9. GABBERT U., TZOU H.S. (Eds.), 2001, *Smart Structures and Structronic Systems*, Kluwer Academic Publishers

10. GABBERT U., WEBER CH.-T., 1999, Optimization of piezoelectric material distribution in smart structures, in Varadan V.V. (Edit.): *Mathematics and Control in Smart Structures, Proceedings of SPIE*, vol. 3667, 13-22

11. GÖRNANDT A., GABBERT U., 2002, Finite element analysis of thermopiezoelectric smart structures, *Acta Mechanica*, **154**, 129-140

12. IRONS B.M., 1976, The semiloof shell element, in Ashwell D.G. and Gallagher R.H. (Eds.): *Finite Elements for Thin Shells and Curved Members*, J. Wiley, London

13. KAMLAH M., TSAKMAKIS C., 1999, Phenomenological modeling of the nonlinear electromechanical coupling in ferroelectrics, *Int. J. of Solids and Structures*, **36**, 669-695

14. KÖPPE H., GABBERT U., TZOU H.-S., 1998, On three-dimensional layered shell elements for the simulation of adaptive structures, in *Fortschr.-Ber. VDI Reihe 11*, 268, Düsseldorf, VDI Verlag, 103-114

15. KÖPPE H., GABBERT U., LAUGWITZ F., WEBER C-T., 1999, Comparison of numerical and experimental results of structronik plate and shell structures, *Computer Assisted Mechanics and Engineering Sciences*, **6**, 361-368

16. LEVIN V.M., RAKOVSKAJA M.I., KREHER W.S., 1999, The effective thermoelectroelastic properties of microinhomogeneous materials, *Int. J. Solids and Structures*, **36**, 2683-2705

17. LIN M.W., ABATAN A.O., ROGERS C.A., 1994, Application of commercial finite element codes for the analysis of induced strain-actuated structures, *Proceedings of 2nd Int. Conference on Intelligent Materials*, June 5-8, 1994, Williamsburg (USA), 846-855

18. SEEGER F., KÖPPE H., GABBERT U., 2001, Analysis and design of smart laminated shell structures, *Proc. of the Colloquium of the ADAMES-Project*, Mai 2001, *Preprints of the INK-ADAMES* (Ed.: U. Gabbert), Otto-von-Guericke-University of Magdeburg, 97-107

19. SPORN D., SCHOENECKER A., 1999, Composites with piezoelectric thin fibers – first evidence of piezoelectric behaviour, *Mat. Res. Innovat.*, **2**, 303-308

20. TIERSTEN H.F., 1969, *Linear Piezoelectric Plate Vibration*, Plenum Press, New York

21. TZOU H.S., 1993, *Piezoelectric Shells (Distributed Sensing and Control of Continua)*, Kluwer Academic Publishers, Dordrecht/Boston/London

22. TZOU H.-S., GURAN A. (EDS.), GABBERT U., TANI J., BREITBACH A. (ASSOCIATE EDS.), 1998, *Structronic Systems: Smart Structures, Devices and Systems*, Vol. 2: *Systems and Control*, World Scientific Publishing Co., New Jersey/Singapore

Modelowanie "inteligentnych" powłok kompozytowych

Sreszczenie

Ostatnie osiągnięcia w dziedzinie konstrukcji "inteligentnych" zwracają uwagę na zastosowanie cienkich folii i włókien piezoelektrycznych o grubości 10-30 μm jako czujników i elementów wykonawczych w aktywnych kompozytach. W pracy zawarto matematyczną analizę i wyniki symulacji numerycznych dla takich właśnie kompozytów. Wprowadzono koncepcję powłokowych laminowanych elementów skończonych z warstwami aktywnymi i pasywnymi oraz zaproponowano trzy różne podejścia, których możliwość zastosowania i przydatność przedyskutowano dla badanego przypadku. Przy weryfikacji adekwatności zaprezentowanego algorytmu do analizy aktywnych układów kompozytowych posłużono się praktycznym przykładem laminatu zawierającego włókna piezoelektryczne osadzone w materiale osnowy. Początkowo użyto wprowadzone powłokowe elementy skończone, gdzie włókna piezoelektryczne zamodelowano jako aktywne warstwy w formie rozmytej. Następnie zastosowano koncepcję układu dyskretnego, w którym włókna piezoelektryczne przedstawiono w formie jednowymiarowych kratowo-podobnych elementów skończonych wbudowanych w konwencjonalne elementy skończone przy użyciu techniki funkcji kary. Te dwie metody przedyskutowano i porównano.

Manuscript received January 3, 2002; accepted for print March 4, 2002